DEGRADANT CHARACTERIZATION REPORT

Document No:	RC-036	**Page:**	1 of 27
Project Number:	8106	**Report No:**	LD1967
Name:	Structural Characterization of CC-00280		

REPORT PREPARED BY			
Name	**Department**	**Signature**	**Date**
[redacted]	AMRI-Bothell Research Center	[redacted]	10 Sept 12

REPORT APPROVED BY			
Name	**Department**	**Signature**	**Date**
[redacted]	AMRI-Bothell Research Center	[redacted]	9-10-12
	The Coca-Cola Company		9-10-12

1.0 Abstract

A degradant named CC-00280 was formed upon heating an acidic aqueous solution of CC-00276 and was isolated from this solution. Spectrometric analysis of CC-00280 (13-[(2-*O*-6-deoxy-β-D-glucopyranosyl-3-*O*-β-D-glucopyranosyl-β-D-glucopyranosyl)oxy] *ent*-kaur-16-hydroxy-19-oic acid-[(2-*O* -β-D-glucopyranosyl -3-*O*-β-D-glucopyranosyl-β-D-glucopyranosyl) ester], Lot VSPC-2973-6B by NMR and MS allowed a full assignment of its structure. Evaluation of the data led to the conclusion that this degradant was produced from CC-00276 (Ref. 6.2) by the addition of water to the exocyclic double bond of the aglycone.

2.0 Background

CC-00276 has been degraded using the stress conditions described below, which generated a number of major degradation products. In order to identify these degradants, the compounds were isolated through a series of liquid chromatographic (LC) steps and then characterized by multiple nuclear magnetic resonance spectrometric (NMR) and mass spectrometric (MS) analyses.

3.0 Materials and Methods

Unless otherwise noted, all work was conducted at AMRI, Bothell Research Center, Bothell, Washington.

3.1 CC-00276. A sample of CC-00276, Lot VSPC-2973-6B, was obtained from Pure Circle, Malaysia.

3.2 LC-MS. Mass spectrometry was carried out on a Sciex API2000 triple quadrupole mass spectrometer with a TurbolonSpray ionization source operating in negative ion mode. A Sedere Sedex 75 ELS detector was used operating at 50 °C and 3.5 bar. Analysis of the samples was performed using the following method: Column: Phenomenex Synergi Hydro RP, 4.6 x 250 mm, 4 µm (p/n 00G-4375-E0); Column Temp: 55 °C; Mobile Phase A: H_2O (0.0284% NH_4OAc, 0.0116% HOAc); Mobile Phase B: Acetonitrile; Flow Rate: 1.0 mL/min; Injection volume: 50 µL. Detection was by UV (210 nm), ELSD, and MSD (+ESI *m/z* 200-1450).

Gradient:

Time (min)	%A	%B
0.0	75	25
8.5	75	25
10.0	71	29
16.5	70	30
18.5	66	34
24.5	66	34
26.5	48	52
29.0	48	52

31.0	30	70
37.0	30	70
37.1	75	25
45.0	75	25

3.3 Isolation of CC-00280 by HPLC. The method (HPLC Method 1) used for the isolation of CC-0280 is summarized below. Column: Gemini C_{18} with guard column, 250 x 10 mm, 5 µm (p/n 00G-4435-N0); Column Temp: 25 °C; Mobile Phase A: H_2O; Mobile Phase B: Acetonitrile; Flow Rate: 5.0 mL/min; Injection volume: 300 µL at 10 mg/mL of degradation mixture CC-00276 Lot VSPC-2973-6B prepared in water-acetonitrile (75:25). Detection was by UV (210 nm).

Gradient:

Time (min)	%A	%B
0.0	75	25
20.0	69	31
20.5	50	50
25.0	40	60
25.1	75	25
30.0	75	25

3.4 MS and MS/MS. MS and MS/MS data were generated with a Waters Premier QTof mass spectrometer equipped with an electrospray ionization source. Samples were diluted with H_2O:acetonitrile (1:1) containing 0.1% formic acid and introduced via infusion using the onboard syringe pump. The samples were diluted to yield good s/n which occurred at an approximate concentration of 0.01 mg/mL.

3.5 NMR. The sample was prepared in pyridine-d_5 and NMR data were acquired on a Bruker Avance 500 MHz instrument with a 5 mm inverse detection probe. The spectrum was referenced to the residual solvent signal (δ_H 8.71, δ_C 149.9 for pyridine-d_5).

3.6 Degradation of CC-00276. A 0.1 M phosphoric acid solution was made and adjusted to pH 2.0 with concentrated ammonium hydroxide. Ten mgs of CC-00276 (Lot VSPC-2973-6B) was added to 10 mL of the phosphoric acid solution. The solution was placed on a heat block at 80 °C for 24 hours. A sample of the degradation mixture was analyzed using the LC-MS method described in Section 3.2.

4.0 Results and Discussion

4.1 Isolation and Purification. Isolation of CC-00280 was performed using the CC-00276 degradation mixture that was prepared as described in Section 3.6. This material was analyzed by LC-MS using the LC-MS method (Section 3.2) and the

results are given in Figure 1. The CC-00276 was observed at 11.5 min in the UV (210 nm) chromatogram. The mass spectrum for the CC-00276 peak provided the expected $[M-H]^-$ ion at *m/z* 1290.3. The CC-00280 peak was observed to elute at 7.1 min in the UV chromatogram and showed an $[M-H]^-$ ion at *m/z* 1308.0. Relative to CC-00276 this indicated a net addition of 18 Daltons. HPLC purification was performed using HPLC Method 1 and the peak eluting at 7.86 min was collected over several injections and dried by rotary evaporation under reduced pressure (Figure 2).

4.2 Mass Spectrometry. The results of an LC-MS analysis of the isolated peak are shown in Figure 3 and confirmed that it corresponded to CC-00280. A single peak was observed in the TIC, UV and ELS chromatograms. The mass spectrum of the isolate of CC-00280 showed an $[M-H]^-$ ion at *m/z* 1308.0 suggesting a nominal mass of 1308 Daltons.

The ESI+ TOF mass spectrum acquired by infusing a sample of CC-00280 showed $[M+H]^+$ and $[M+Na]^+$ ions at *m/z* 1309.5588 and 1331.5414, respectively (Figure 4). The mass of the $[M+H]^+$ ion was in good agreement with the molecular formula $C_{56}H_{92}O_{34}$ (calcd for $C_{56}H_{93}O_{34}$: 1309.5548, error: 3.0 ppm) for CC-00280 (Figure 5). The ESI- mass spectrum provided $[M-H]^-$ and $[M+HCOOH-H]^-$ ions at *m/z* 1307.5353 and 1353.5399, respectively (Figure 6). As above, the mass of the $[M-H]^-$ ion was in good agreement with the molecular formula $C_{56}H_{92}O_{34}$ (calcd for $C_{56}H_{91}O_{34}$: 1307.5392, error: -2.8 ppm) for CC-00280 (Figure 7). The +ESI and -ESI data indicated that CC-00280 has a nominal mass of 1308 Daltons with the molecular formula, $C_{56}H_{92}O_{34}$. The molecular formula of CC-00280 differs from that of CC-00276 by the net addition of H_2O.

The +ESI TOF MS/MS spectrum of CC-00280, fragmenting on the $[M+H]^+$ ion at *m/z* 1309 is provided in Figure 8 and showed an ion at *m/z* 1291.5469 corresponding to the loss of H_2O. A series of fragment ions were observed at *m/z* 1147.5048, 985.4510, 823.3992, and 661.3459 due to the sequential loss of 4 glucose moieties. A second series of fragment ions were observed at *m/z* 1129.4951, 967.4416, 805.3882, 643.3328, 481.2800, and 319.2282 due to the sequential loss of 6 glucose moieties from the ion at *m/z* 1291.5469. A fragment ion was also observed at *m/z* 973.3272 corresponding to 6 glucose moieties and this ion underwent sequential loss of 5 glucose residues to yield fragment ions at *m/z* 811.2730, 649.2197, 487.1658, 325.1145, and 163.0630. The fragmentation pattern observed for CC-00280 was very similar to that observed for CC-00276 and indicated the presence of 6 glucose residues.

The -ESI Tof MS/MS spectrum of CC-00280, fragmenting on the $[M-H]^-$ ion at *m/z* 1307 indicated that the most abundant and readily formed ion is present at *m/z* 821.3790 and corresponds to the loss of three glucose residues (Figure 9). This suggested that the glycoside at C-19 is likely composed of three glucose residues and by inference indicated that the glycoside at C-13 also likely is composed of three glucose residues.

4.3 NMR Spectrometry. A series of NMR experiments including ^{1}H NMR (Figure 10), ^{1}H-^{1}H COSY (Figure 11), HSQC (Figure 12), HMBC (Figure 13) were performed to allow the assignment of CC-00280. A preliminary inspection of the NMR data indicated that the olefinic protons observed for CC-00276 were absent. Together with the MS data this suggested that addition of H_2O at the C-16 unsaturation may have occurred during degradation.

An HMBC correlation from the methyl protons at δ_H 1.28 ppm to the carbonyl at δ_C 176.9 allowed assignment of one of the tertiary methyl groups (C-18) as well as C-19 and provided a starting point for assignment of the rest of the aglycone. Additional HMBC correlations from the methyl protons (H-18) to carbons at δ_C 38.4, 43.8, and 57.1 allowed assignment of C3 to C5 in comparison with the data for CC-00276 (Ref 6.2). The ^{1}H chemical shifts for C-3 (δ_H 1.00 and 2.32) and C-5 (δ_H 1.04) were assigned using the HSQC data. A COSY correlation between one of the H-3 protons (δ_H 1.00) and a proton at δ_H 1.34 allowed assignment of one of the H-2 protons which in turn showed a correlation with a proton at δ_H 0.78 which was assigned to C-1. The remaining ^{1}H and ^{13}C chemical shifts for C-1 and C-2 were then assigned on the basis of additional COSY and HSQC correlations and are summarized in Table 1.

Two additional tertiary methyl singlets were observed as a single overlapped singlet at δ_H 1.31 in the ^{1}H NMR spectrum but showed HSQC correlations to separate carbons at δ_C 16.0 and 22.2. One of these overlapped singlets (δ_H 1.31, δ_C 16.0) was tentatively assigned as C-20 in comparison with the data for CC-00276 and showed HMBC correlations to C-1 and C-5. The methyl protons showed an additional HMBC correlation to a methine (δ_H 0.84, δ_C 54.8) which was assigned as C-9. An HMBC correlation between H-9 and a carbon at δ_C 16.0 then confirmed the assignment of the C-20 methyl group. COSY correlations between H-5 (δ_H 1.04) and protons at δ_H 2.11 and 2.43 then allowed assignment of the H-6 protons which in turn showed correlations to protons at δ_H 1.37 and 1.88 which were assigned to C-7. The ^{13}C chemical shifts for C-6 (δ_C 23.1) and C-7 (δ_C 42.8) were then determined from the HSQC data.

COSY correlations between H-9 (δ_H 0.84) and protons at δ_H 1.52 and 1.71 allowed assignment of the H-11 protons which in turn showed COSY correlations to protons at δ_H 1.85 and 2.67 which were assigned as the H-12 protons. The HSQC data was then used to assign C-11 (δ_C 19.8) and C-12 (δ_C 31.6). An HMBC correlation between the H-11 protons and a carbon at δ_C 87.6 allowed assignment of C-13. As noted above signals for the olefinic H-17 protons were not observed. The remaining methyl singlet (δ_H 1.31, δ_C 22.2) showed an HMBC correlation to C-13 and was assigned to C-17. Additional HMBC correlations between the H-17 protons and carbons at δ_C 54.3 and 77.1 then allowed assignment of C-15 and C-16, respectively. The ^{13}C chemical shift for C-16 indicated substitution with a hydroxyl group at this position. The H-15 protons (δ_H 1.41 and 1.83) were assigned from the HSQC data and showed HMBC correlations to C-9, C-16 and a carbon at δ_C 40.3 which was assigned as C-14.

The ^{1}H chemical shifts for the H-14 protons (δ_H 2.44 and 2.58) were assigned from the HSQC data. Additional HMBC correlations between H-9 and C-12, C-14, and C-15 confirmed their assignments.

Analysis of the NMR data for the aglycone, together with MS data, indicated that addition of H_2O had occurred at C-16 with concomitant loss of the double bond. An analogous degradant (CC-00207) was isolated from a degradation preparation of Rebaudioside A (CC-00201) in a previous study (Ref. 6.3). A summary of the ^{1}H and ^{13}C chemical shifts for the aglycone are found in Table 1 and a summary of the key HMBC and COSY correlations used to assign the aglycone region are provided in Figure 14.

An analysis of the HSQC data for CC-00280 confirmed the presence of 6 anomeric positions. Four of the anomeric protons were well resolved at δ_H 6.35 (δ_C 94.5), 5.63 (δ_C 103.8), 5.53 (δ_C 103.8), and 5.22 (δ_C 104.0) in the ^{1}H NMR spectrum. The remaining two anomeric protons were observed at δ_H 5.79 (δ_C 96.0) and 5.76 (δ_C 104.0) and were partially overlapped in the ^{1}H NMR spectrum. The anomeric proton observed at δ_H 6.35 showed an HMBC correlation to C-19 which indicated that it corresponds to the anomeric proton of Glc_I. The anomeric proton observed at δ_H 5.79 was assigned as the anomeric proton of Glc_{II} in comparison with CC-00276.

The Glc_I anomeric proton (δ_H 6.35) showed a COSY correlation to a proton at δ_H 4.53 which was assigned as Glc_I H-2 and in turn showed a COSY correlation to a proton at δ_H 4.98 (Glc_I H-3) which showed a correlation with a proton at δ_H 4.21 (Glc_I H-4). Assignment of the ^{13}C chemical shifts for Glc_I C-2 (δ_C 76.4), C-3 (δ_C 88.5), and C-4 (δ_C 69.7) was made using the HSQC data. The assignments at Glc_I C-5 and C-6 were made using the ^{1}H and HSQC data in comparison with the data for CC-00276.

Assignment of Glc_{II} was carried out in a similar manner. The Glc_{II} anomeric proton (δ_H 5.79) showed a COSY correlation to a proton at δ_H 4.14 which was assigned as Glc_{II} H-2 and in turn showed a COSY correlation to a proton at δ_H 5.09 (Glc_{II} H-3) which showed an additional correlation with a proton at δ_H 4.00 (Glc_{II} H-4). Assignment of the ^{13}C chemical shifts for Glc_{II} C-2 (δ_C 80.4), C-3 (δ_C 87.9), and C-4 (δ_C 69.9) was then completed using the HSQC data. The assignments at Glc_{II} C-5 and C-6 were made using the ^{1}H, COSY and HSQC data in comparison with the data for CC-00276.

Two of the remaining unassigned glucose moieties were assigned as substituents at C-2 and C-3 of Glc_I on the basis of HMBC correlations. The anomeric proton observed at δ_H 5.76 showed an HMBC correlation to Glc_I C-2 and was assigned as the anomeric proton of Glc_V. The anomeric proton observed at δ_H 5.22 showed an HMBC correlation to Glc_I C-3 and was assigned as the anomeric proton of Glc_{VI}. The reciprocal HMBC correlation between Glc_I H-2 and anomeric carbon of Glc_V was also observed. The assignments for C-2

through C-6 of Glc_V and Glc_{VI} were made using the ^1H, COSY and HSQC data in comparison with the assignment of CC-00276.

A summary of the ^1H and ^{13}C chemical shifts for the glycoside at C-19 are found in Table 2 and a summary of the key HMBC and COSY correlations used to assign the C-19 glycoside region are provided in Figure 15.

The two remaining unassigned sugar moieties were assigned as substituents at C-2 and C-3 of Glc_{II} on the basis of HMBC correlations. The anomeric proton observed at δ_H 5.63 showed an HMBC correlation to Glc_{II} C-2 and was assigned as the anomeric proton of Glc_{III}. The anomeric proton observed at δ_H 5.53 showed an HMBC correlation to Glc_{II} C-3 and was assigned as the anomeric proton of Glc_{IV}. The reciprocal HMBC correlation between Glc_{II} H-2 and the anomeric carbon of Glc_{III} was also observed. The assignments for C-2 through C-6 of Glc_{III} and Glc_{IV} were made using the ^1H, COSY and HSQC data in comparison with the assignment of CC-00276.

A summary of the ^1H and ^{13}C chemical shifts for the glycoside at C-13 are found in Table 3 and a summary of the key HMBC and COSY correlations used to assign the C-13 glycoside region are provided in Figure 16. The NMR data for the glycoside regions showed that they were unchanged relative to CC-00276. The structure of CC-00280 is shown in Figure 17.

4.4 Chromatography. When analyzed under the conditions of the LC/MS method described above, CC-00280 had a retention time of 7.1 min.

5.0 Conclusions

NMR and MS analyses of CC-00280 allowed a full assignment of its structure. The chemical name of CC-00280 is 13-[(2-*O*-6-deoxy-β-D-glucopyranosyl-3-*O*-β-D-glucopyranosyl-β-D-glucopyranosyl)oxy] *ent*-kaur-16-hydroxy-19-oic acid-[(2-*O*-β-D-glucopyranosyl -3-*O*-β-D-glucopyranosyl-β-D-glucopyranosyl) ester].

6.0 References

6.1 AMRI-Bothell Research Center Notebook # 833 pp. 1-3, 45, 48-57

6.2 RC-032 "Structural Characterization of CC-00276"

6.3 RC-002 "Isolation and Identification of CC-00207 (DAQ 1)"

7.0 Appendices and Attachments

7.1 Figure 1. LC-MS analysis of CC-00276 Lot VSPC-2973-6B degradation preparation showing TIC (**A**), mass spectrum of the CC-00276 peak at 11.5 min (**B**), mass spectrum of the CC-00280 peak at 7.1 min (**C**) and UV (210 nm) chromatogram (**D**).

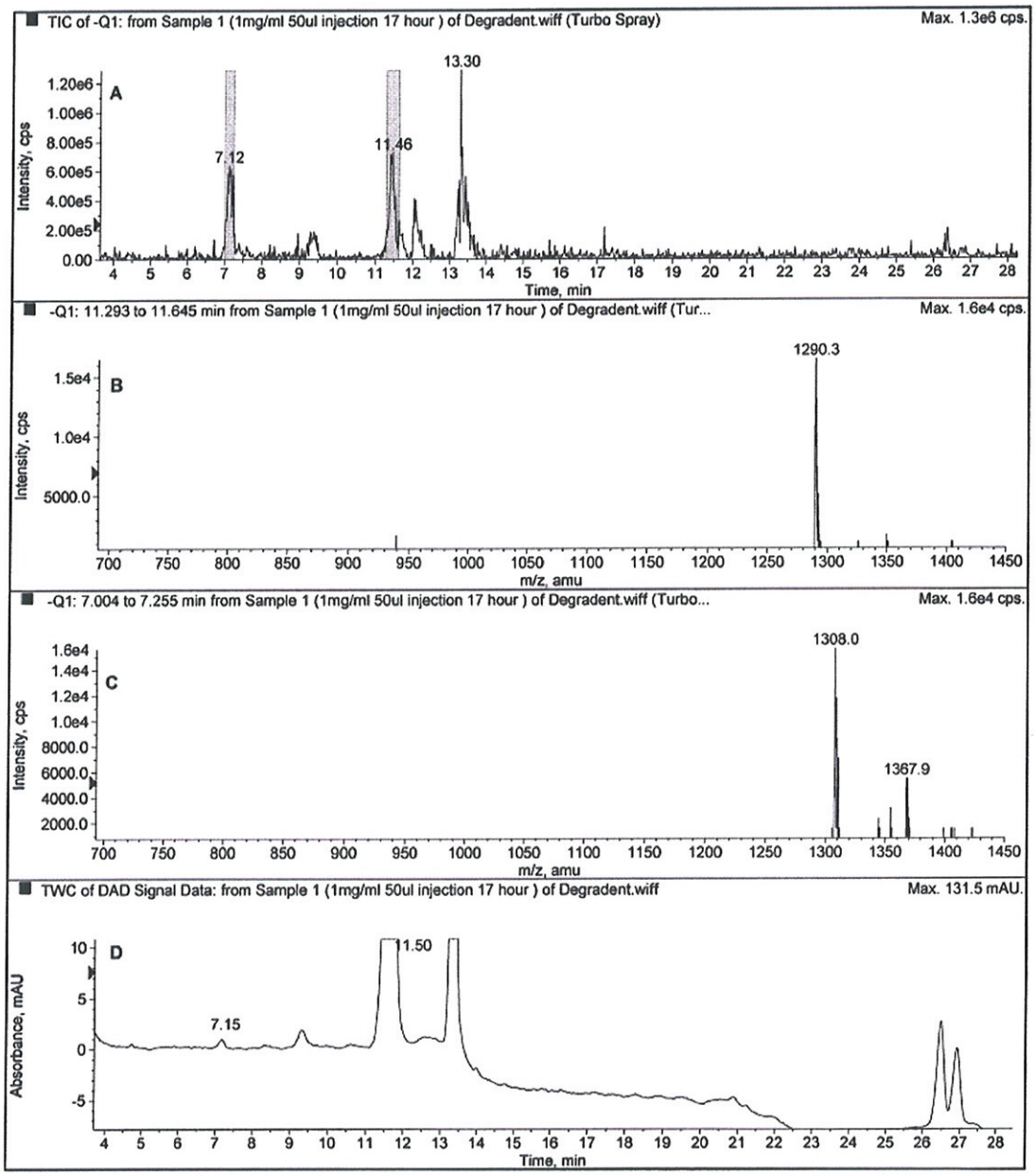

7.2 Figure 2. Representative HPLC UV (210 nm) chromatogram for CC-00276 Lot VSPC-2973-6B degradation preparation.

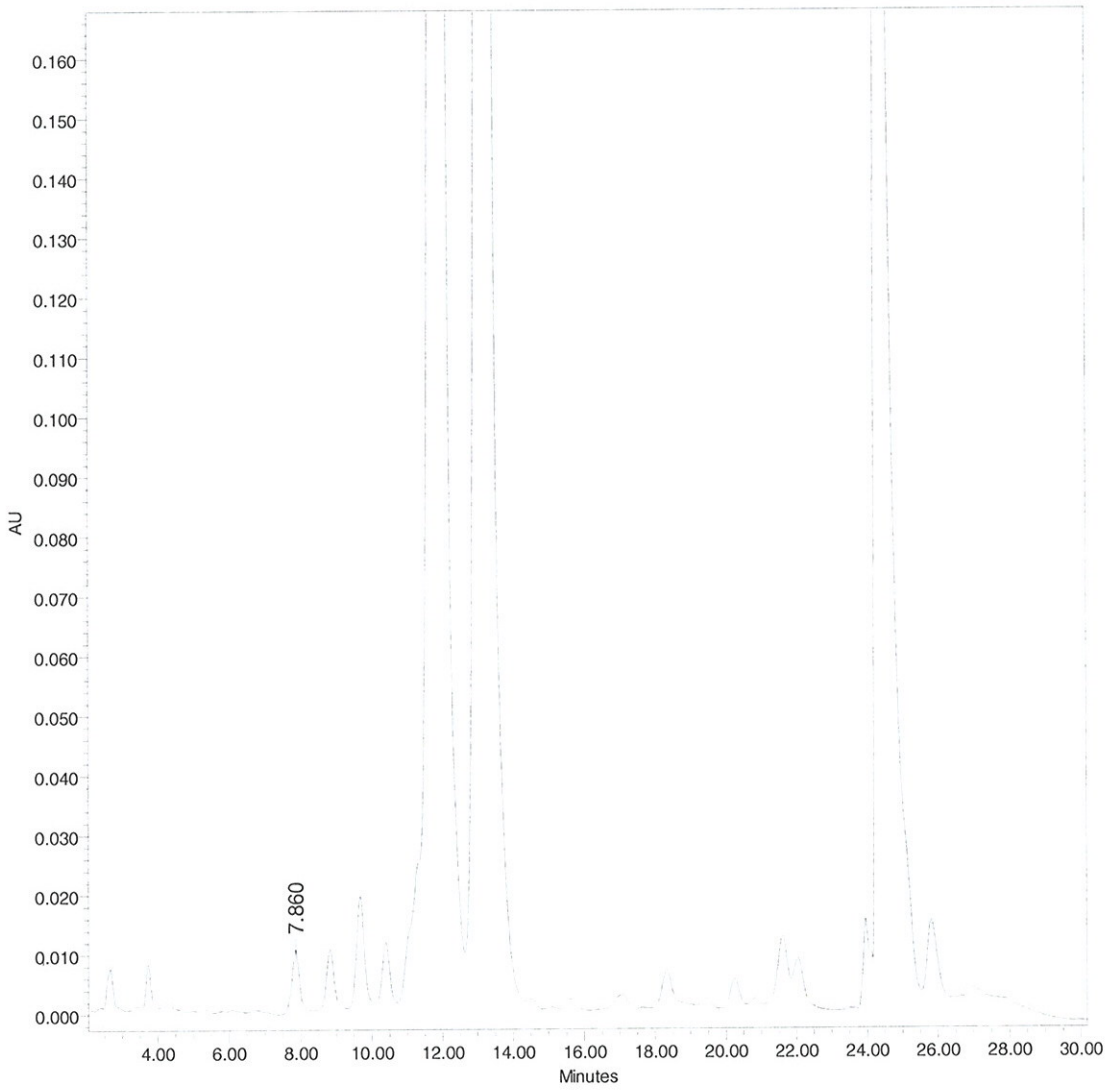

7.3 Figure 3. LC-MS analysis of isolated sample of CC-00280 showing TIC (**A**), mass spectrum of the CC-00280 peak at 7.3 min (**B**), UV (210 nm) chromatogram (**C**) and ELS chromatogram (**D**).

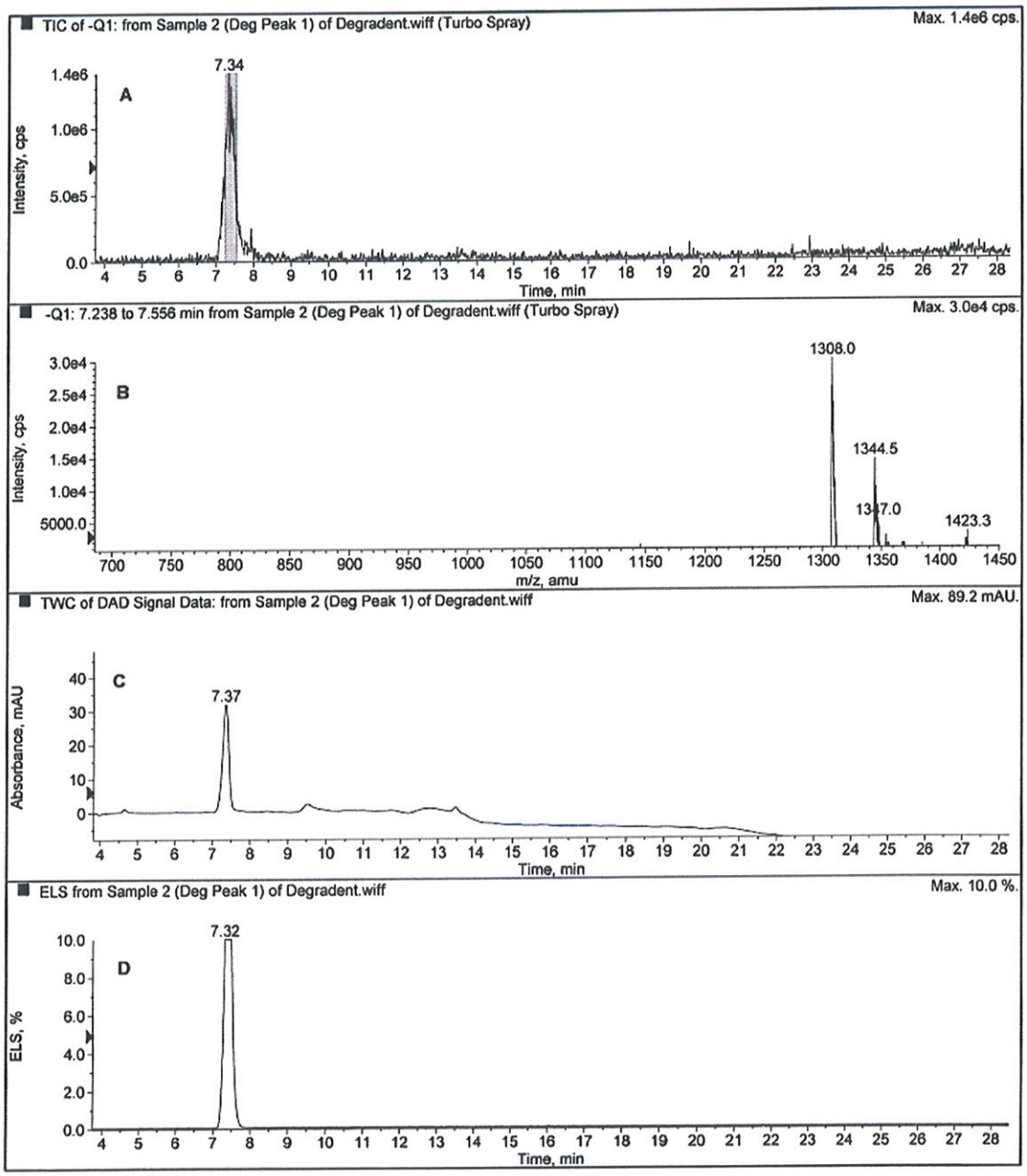

7.4 Figure 4. ESI+ TOF mass spectrum of CC-00280.

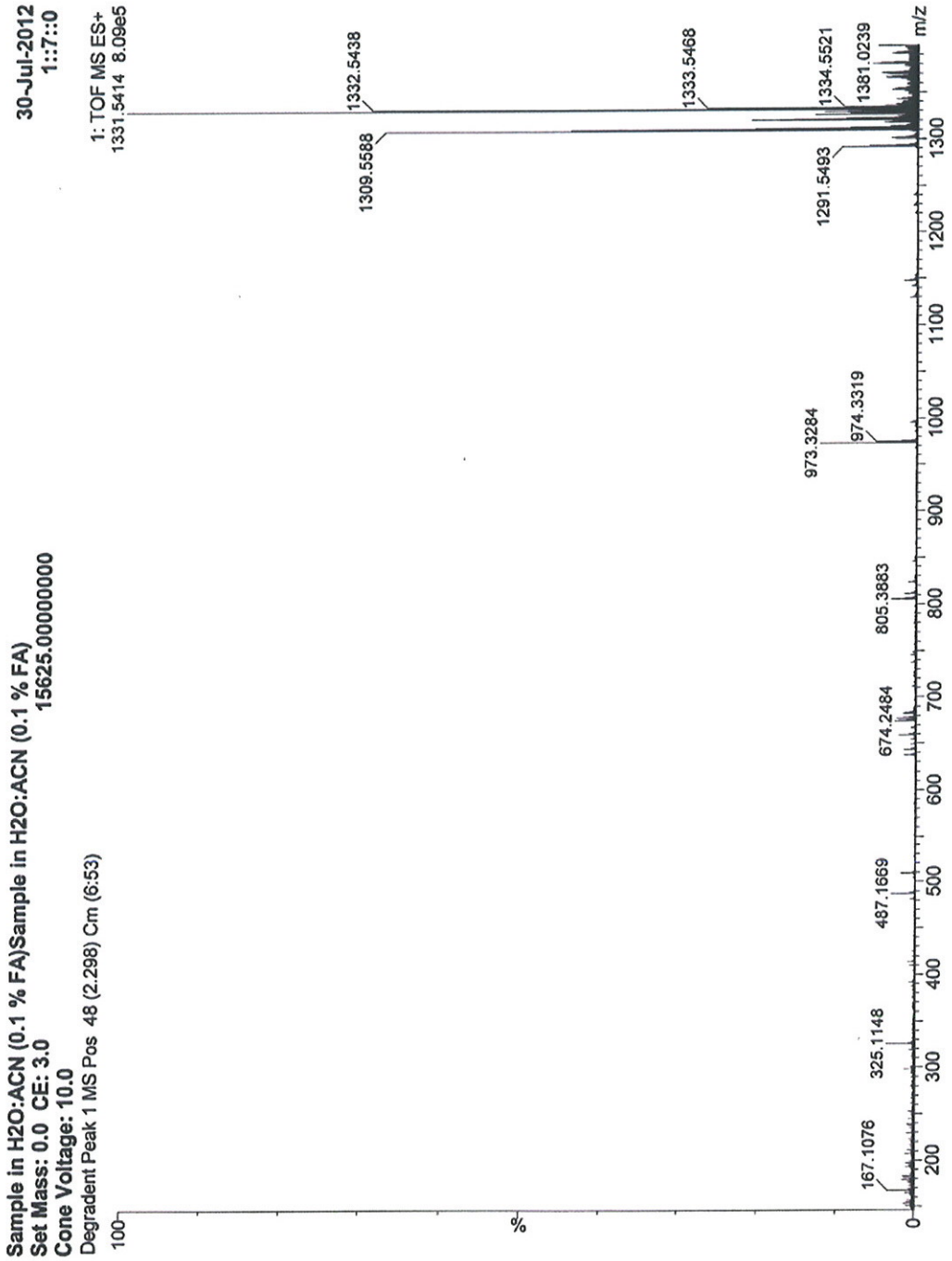

7.5 Figure 5. Accurate mass analysis of the $[M+H]^+$ ion of CC-00280.

Single Mass Analysis
Tolerance = 5.0 PPM / DBE: min = -1.5, max = 50.0
Selected filters: None

Monoisotopic Mass, Even Electron Ions
91 formula(e) evaluated with 2 results within limits (up to 50 closest results for each mass)
Elements Used:
C: 0-60 H: 0-101 O: 0-40

Sample in H2O:ACN (0.1 % FA)Sample in H2O:ACN (0.1 % FA)
Set Mass: 0.0 CE: 3.0
Cone Voltage: 10.0
Degradent Peak 1 MS Pos 48 (2.298) Cm (1:54)
15625.00000000
30-Jul-2012
1::7::0
1: TOF MS ES+
6.11e5

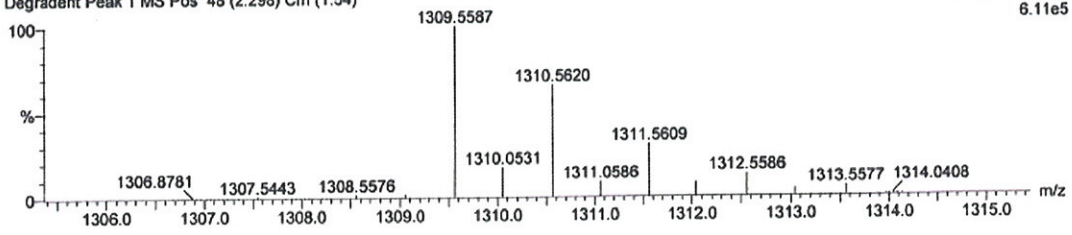

Minimum:				-1.5		
Maximum:		3.0	5.0	50.0		
Mass	Calc. Mass	mDa	PPM	DBE	i-FIT	Formula
1309.5587	1309.5548	3.9	3.0	10.5	724.3	C56 H93 O34
	1309.5607	-2.0	-1.5	1.5	4482.2	C49 H97 O39

7.6 Figure 6. ESI- TOF mass spectrum of CC-00280.

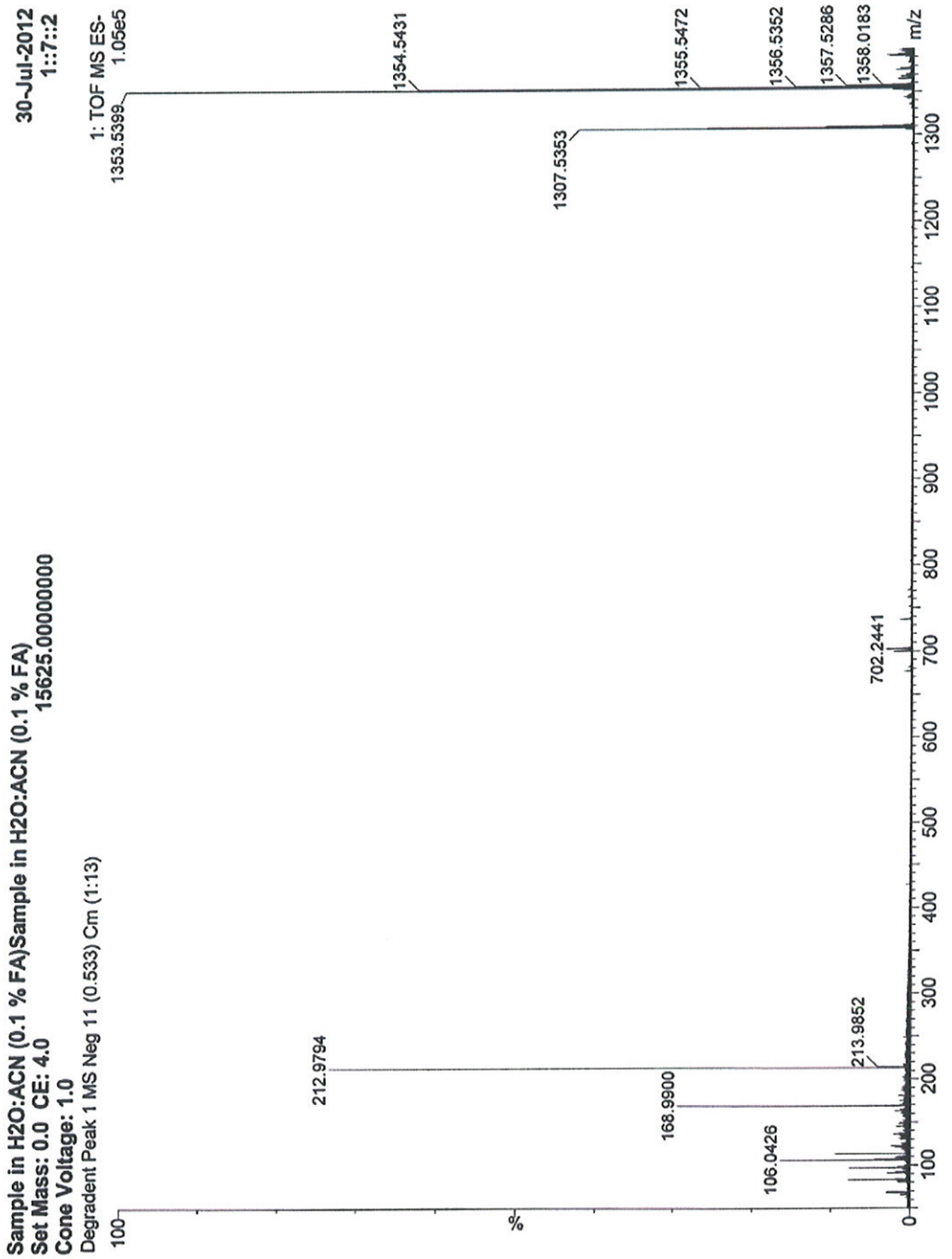

7.7 Figure 7. Accurate mass analysis of the $[M-H]^-$ ion of CC-00280.

Single Mass Analysis
Tolerance = 5.0 PPM / DBE: min = -1.5, max = 50.0
Selected filters: None

Monoisotopic Mass, Even Electron Ions
91 formula(e) evaluated with 1 results within limits (up to 50 closest results for each mass)
Elements Used:
C: 0-60 H: 0-101 O: 0-40

Sample in H2O:ACN (0.1 % FA)Sample in H2O:ACN (0.1 % FA)
Set Mass: 0.0 CE: 4.0
Cone Voltage: 1.0
Degradent Peak 1 MS Neg 11 (0.533) Cm (4:12)
15625.00000000
30-Jul-2012
1::7::2
1: TOF MS ES-
3.10e4

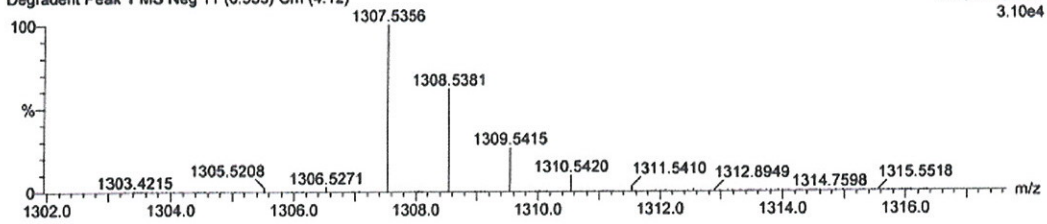

Minimum:				-1.5		
Maximum:		3.0	5.0	50.0		
Mass	Calc. Mass	mDa	PPM	DBE	i-FIT	Formula
1307.5356	1307.5392	-3.6	-2.8	11.5	21.4	C56 H91 O34

7.8 Figure 8. ESI+ TOF MS/MS analysis of CC-00280 selecting the $[M+H]^+$ ion at *m/z* 1309 for fragmentation.

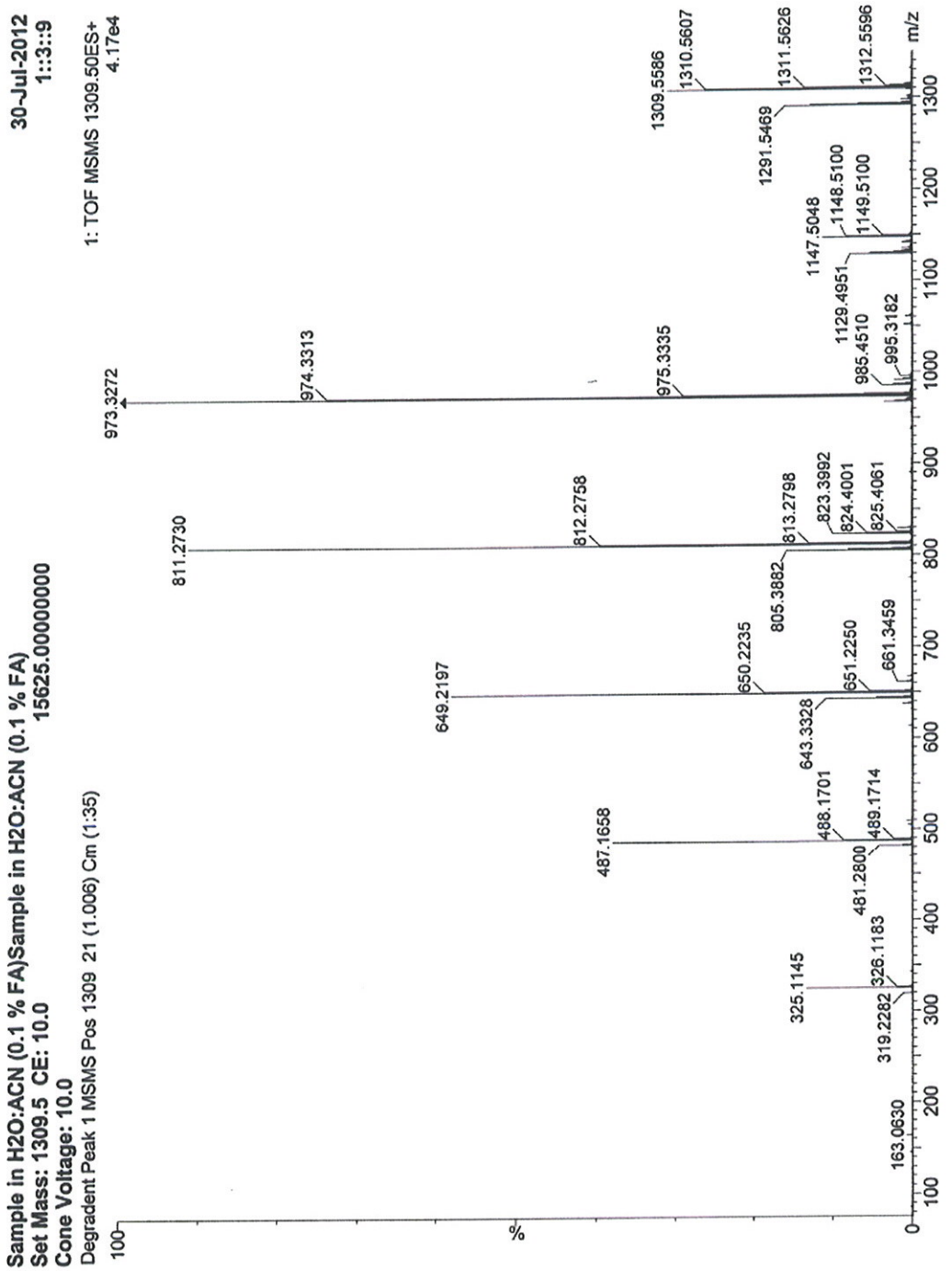

7.9 Figure 9. ESI- TOF MS/MS analysis of CC-00280 selecting the $[M-H]^-$ ion at *m/z* 1307 for fragmentation

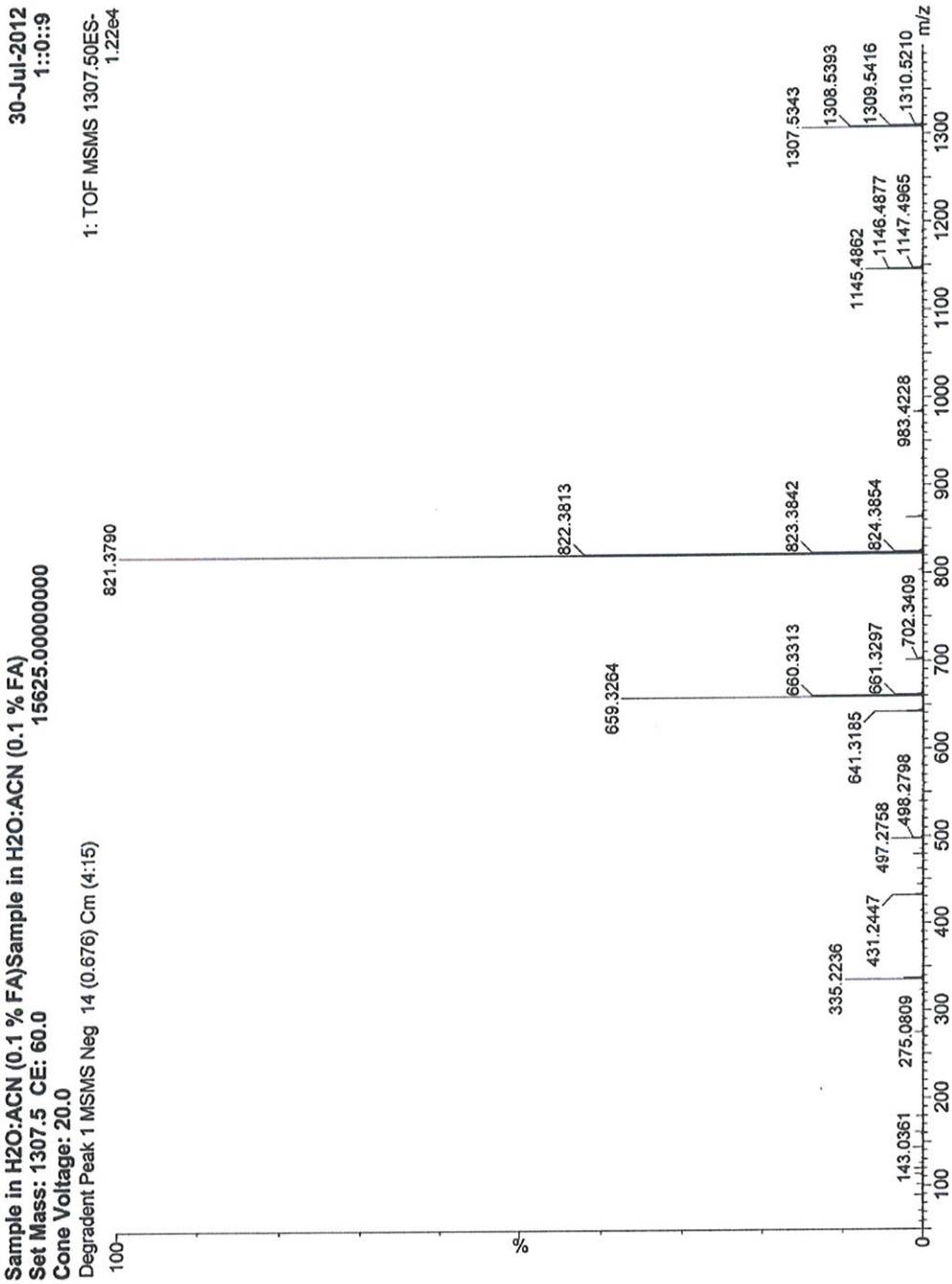

7.10 Figure 10. ^{1}H NMR (500 MHz, pyridine-d_5) of CC-00280.

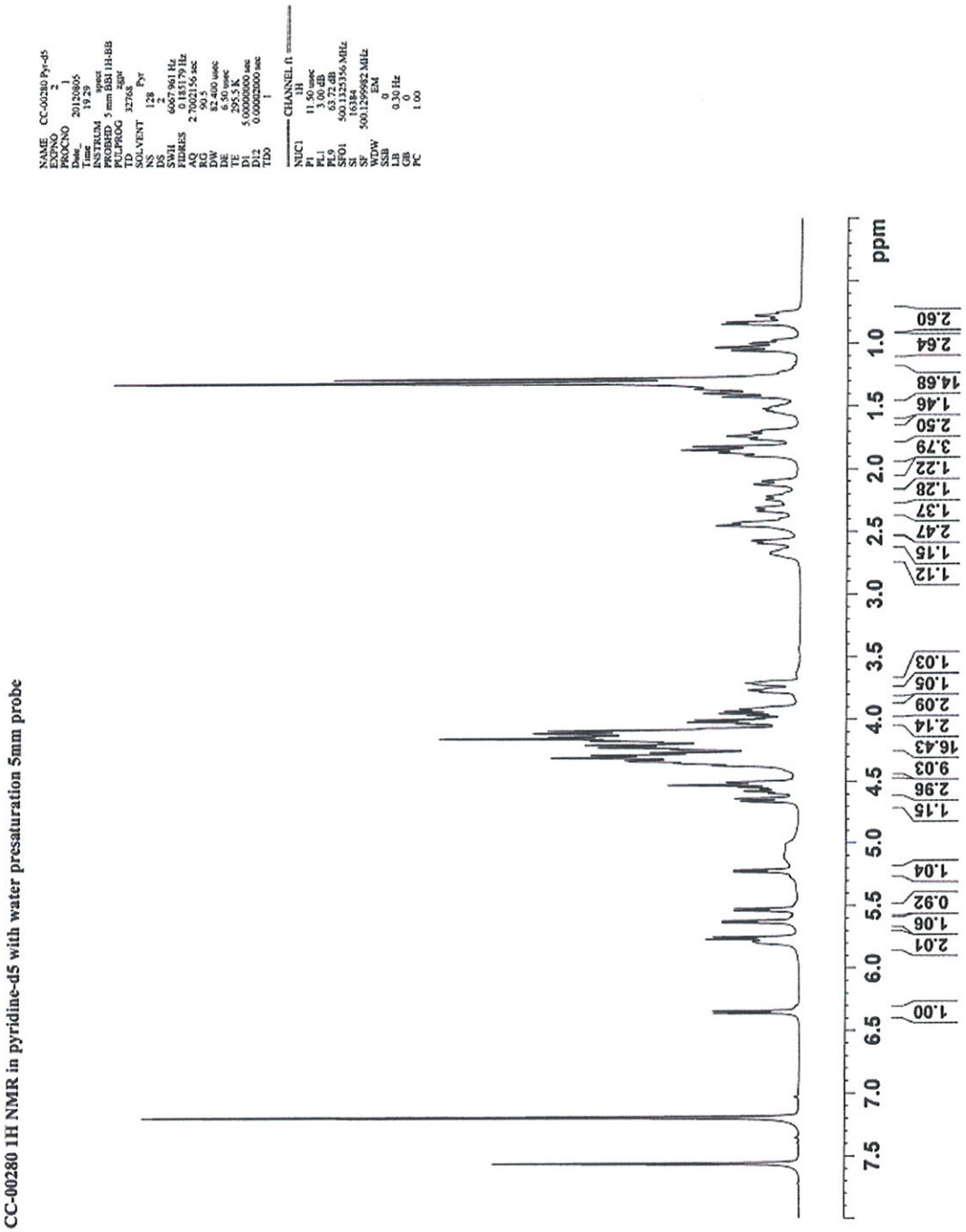

7.11 Figure 11. ^{1}H-^{1}H COSY Spectrum (500 MHz, pyridine-d_5) of CC-00280.

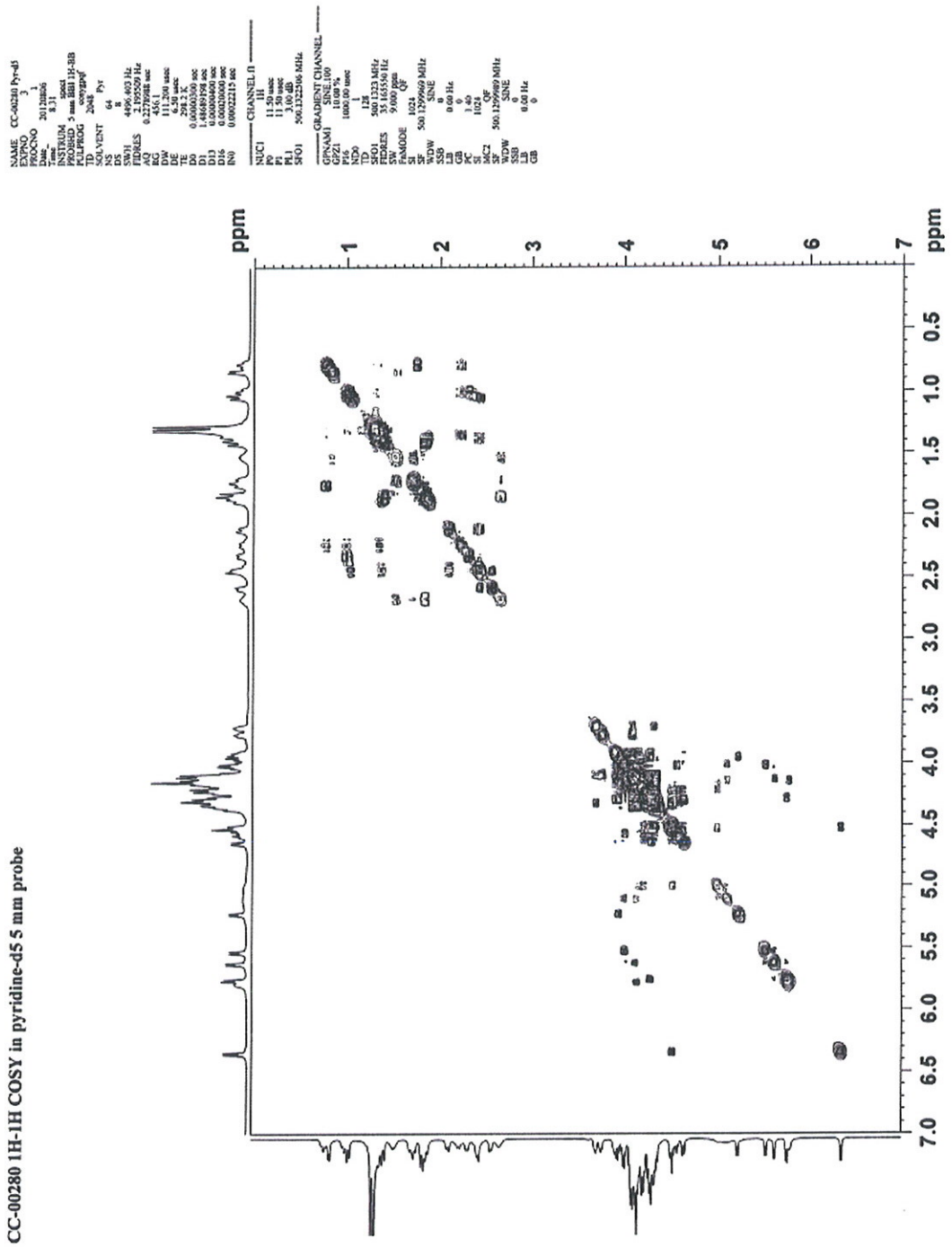

7.12 Figure 12. HSQC Spectrum (500 MHz, pyridine-d_5) of CC-00280.

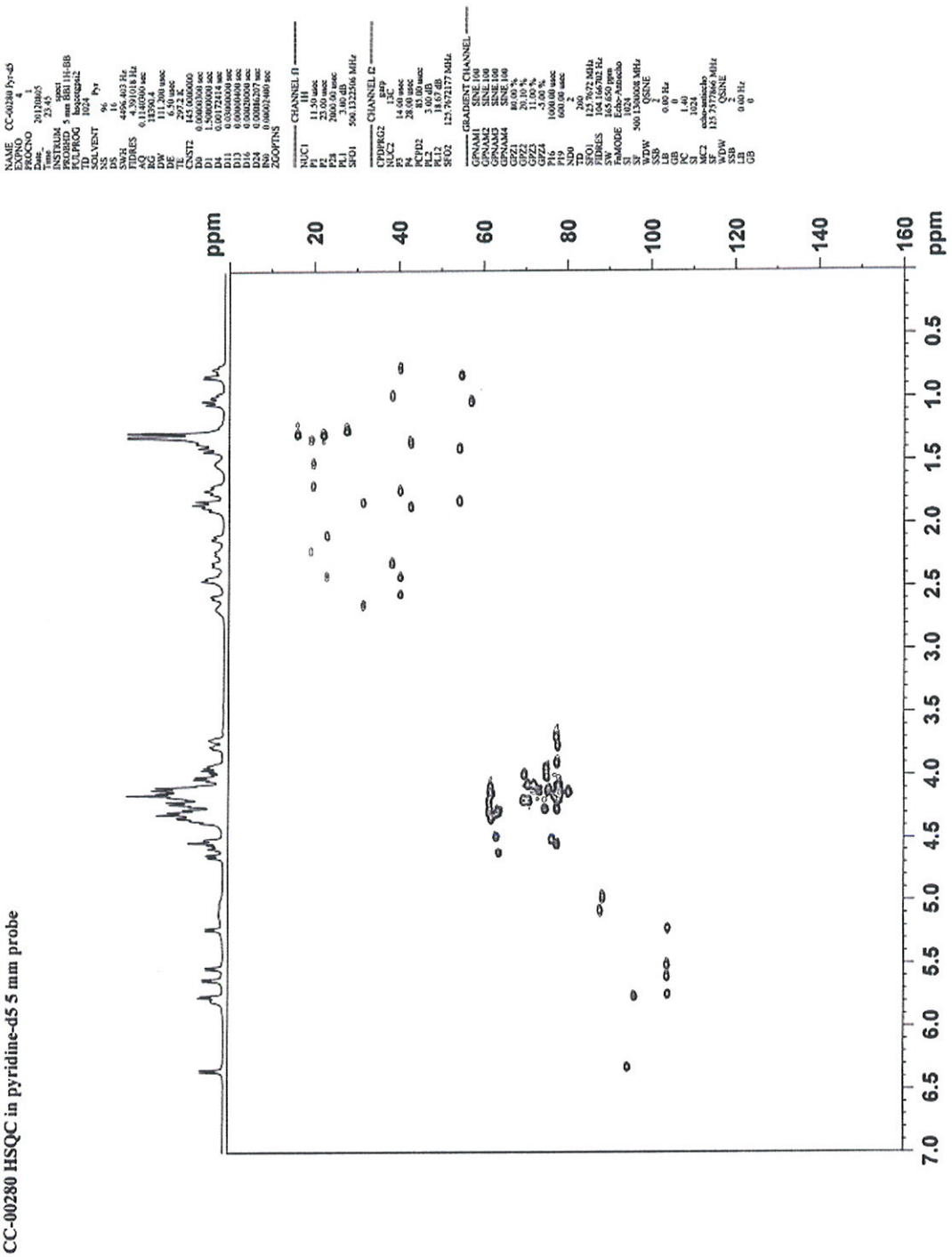

7.13 Figure 13. HMBC Spectrum (500 MHz, pyridine-d_5) of CC-00280.

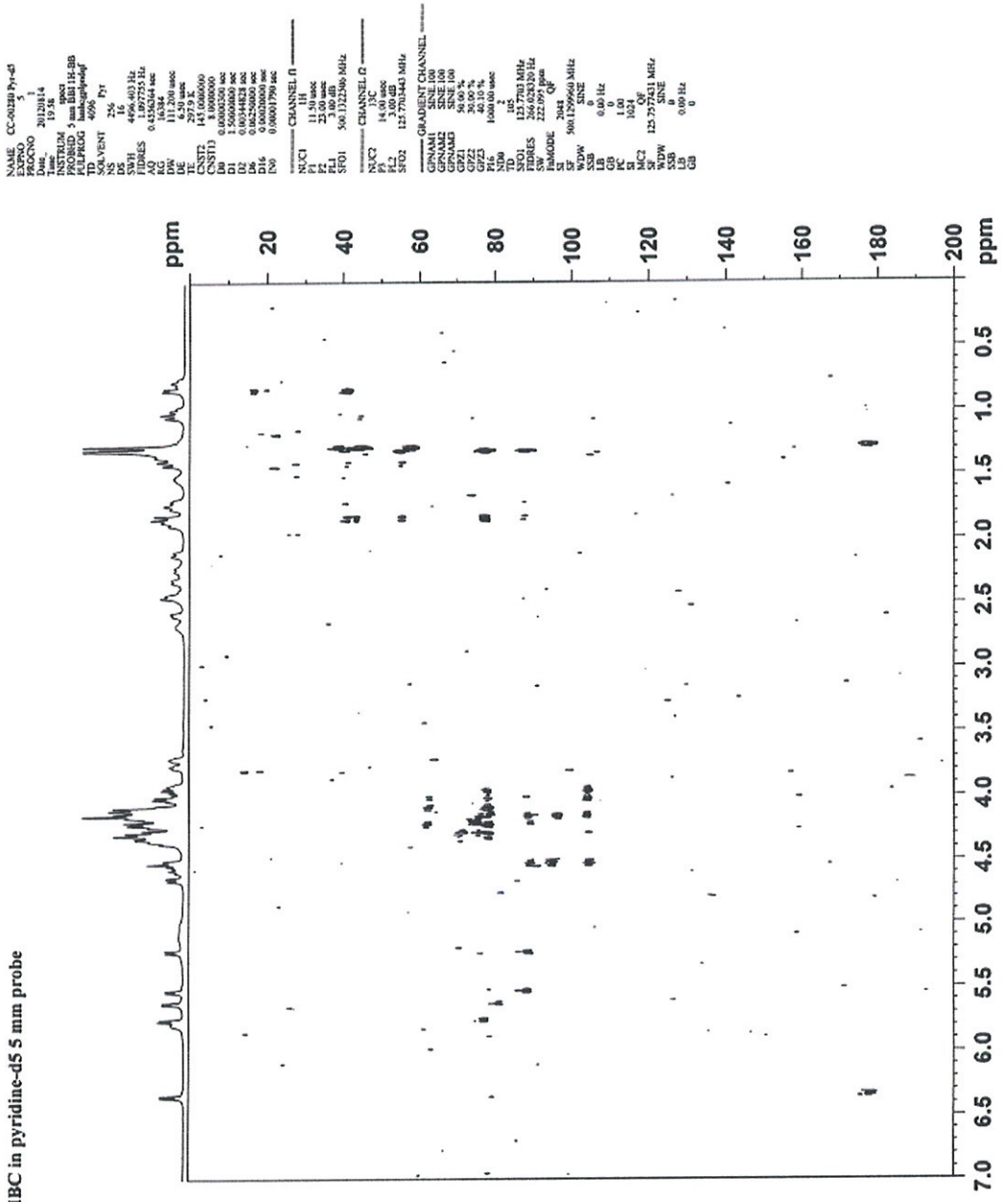

7.14 Figure 14. Summary of Key HMBC and COSY correlations used to assign the aglycone region of CC-00280.

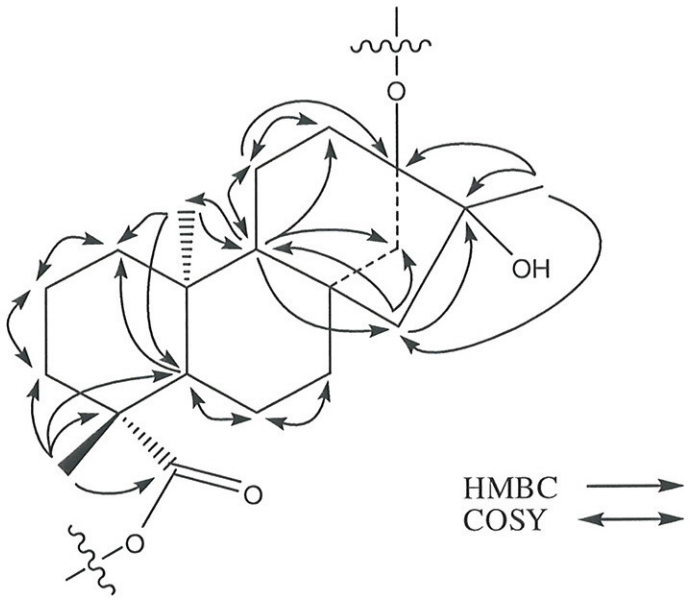

7.15 Figure 15. Summary of Key HMBC and COSY correlations used to assign the C-19 glycoside region of CC-00280.

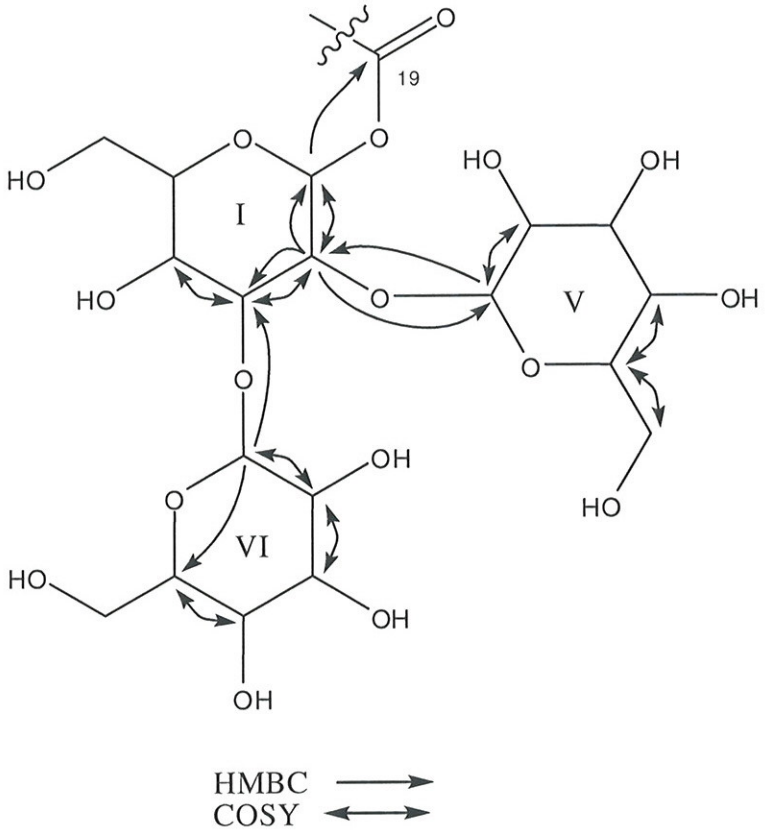

7.16 Figure 16. Summary of Key HMBC and COSY correlations used to assign the C-13 glycoside region of CC-00280.

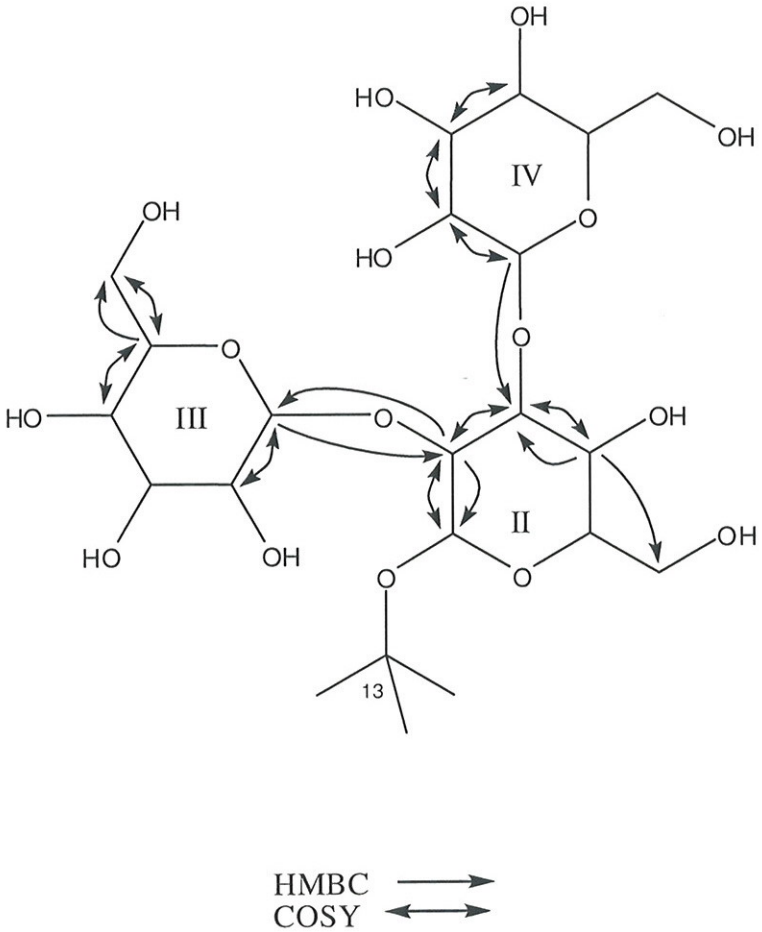

7.17 Figure 17. Structure of CC-00280.

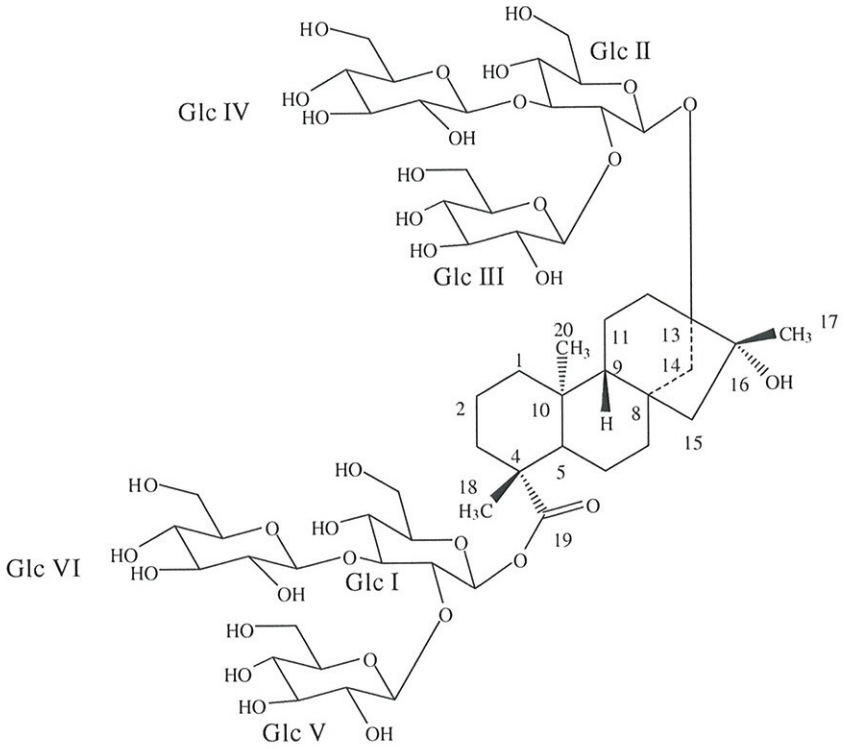

CC-00280

7.18 Table 1. ^{1}H and ^{13}C NMR (500 and 125 MHz, pyridine-d_5) Assignments of the CC-00280 aglycone.

	CC-00280	
Position	^{13}C	^{1}H
1	40.3	0.78 t (13.2) 1.75 d (13.0)
2	19.3	1.34 m 2.23 m
3	38.4	1.00 td (3.9, 12.8) 2.32 d (12.3)
4	43.8	---
5	57.1	1.04 d (12.7)
6	23.1	2.11 d (13.5) 2.43 m
7	42.8	1.37 m 1.88 m
8		---
9	54.8	0.84 d (8.1)
10		---
11	19.8	1.52 m 1.71 m
12	31.6	1.85 m 2.67 m
13	87.6	---
14	40.3	2.44 m 2.58 d (9.9)
15	54.3	1.41 d (14.3) 1.83 m
16	77.1	---
17	22.2	1.31 s
18	27.7	1.28 s
19	176.9	---
20	16.0	1.31 s

7.19 Table 2. ^{1}H and ^{13}C NMR (500 and 125 MHz, pyridine-d_5) Assignments of the CC-00280 C-19 glycoside.

	CC-00280	
Position	^{13}C	^{1}H
Glc_I-1	94.5	6.35 d (8.3)
Glc_I-2	76.4	4.53 t (8.7)
Glc_I-3	88.5	4.98 m
Glc_I-4	69.7	4.21 m
Glc_I-5	78.3	4.14 m
Glc_I-6	61.5	4.22 m 4.30 m
Glc_V-1	104.0	5.76 d (7.8)
Glc_V-2	74.8	4.28 m
Glc_V-3	78.1	4.20 m
Glc_V-4	73.5	4.13 m
Glc_V-5	77.6	3.92
Glc_V-6	63.8	4.29 m 4.64 dd (2.6, 11.6)
Glc_{VI}-1	104.0	5.22 d (7.8)
Glc_{VI}-2	75.1	3.95 m
Glc_{VI}-3	77.7	4.28 m
Glc_{VI}-4	70.8	4.08 m
Glc_{VI}-5	77.8	3.76 m
Glc_{VI}-6	62.0	4.13 m 4.34 m

7.20 Table 3. ^{1}H and ^{13}C NMR (500 and 125 MHz, pyridine-d_5) Assignments of the CC-00279 C-13 glycoside.

	CC-00279	
Position	^{13}C	^{1}H
Glc_{II}-1	96.0	5.79 d (6.7)
Glc_{II}-2	80.4	4.14 m
Glc_{II}-3	87.9	5.09 m
Glc_{II}-4	69.9	4.00 m
Glc_{II}-5	77.2	4.17 m
Glc_{II}-6	62.0	4.13 m 4.34 m
Glc_{III}-1	103.8	5.63 d (7.3)
Glc_{III}-2	75.6	4.13 m
Glc_{III}-3	78.0	4.09 m
Glc_{III}-4	72.2	4.08 m
Glc_{III}-5	77.5	3.70 m
Glc_{III}-6	63.2	4.32 m 4.49m
Glc_{IV}-1	103.8	5.53 d (7.9)
Glc_{IV}-2	75.3	4.02 m
Glc_{IV}-3	77.6	4.55 t (9.0)
Glc_{IV}-4	71.0	4.22 m
Glc_{IV}-5	78.0	4.09 m
Glc_{IV}-6	62.0	4.13 m 4.34 m